Available online at www.sciencedirect.com
ScienceDirect
Scripta Materialia 61 (2009) 640–643
Scripta MATERIALIA
www.elsevier.com/locate/scriptamat

Stress-induced structural inhomogeneity and plasticity of bulk metallic glasses

H.B. Yu,[a] J. Hu,[b] X.X. Xia,[a] B.A. Sun,[a] X.X. Li,[b] W.H. Wang[a] and H.Y. Bai[a,*]

[a]*Institute of Physics, Chinese Academy of Sciences, Beijing 100190, China*
[b]*School of Mechanical Engineering and Automation, Beihang University, Beijing 100191, China*

Received 11 April 2009; revised 28 May 2009; accepted 1 June 2009
Available online 6 June 2009

The correlation between stress-induced structural inhomogeneity and plasticity in bulk metallic glasses (BMGs) was studied. It was found that the structural inhomogeneity induced by an appropriate stress field can markedly enhance macroscopic compressive plasticity in various monolithic BMGs. The origin for the plasticization is correlated to the size of the plastic zone of BMGs.

Keywords: Metallic glass, Microstructure; Ductility

Bulk metallic glasses (BMGs) possess excellent mechanical properties, such as a high elastic limit, high strength and toughness [1–3]. However, their applications as structural materials are restricted by their brittleness at room temperature [3–5]. The brittleness also hinders studies on a number of fundamental issues, such as the deformation mechanism [6] and serrated flow [7] in glasses. Considerable efforts have been made [8–18] to ductilize BMGs, and microstructural inhomogeneity is an effective approach [9–13]. This kind of structure consists of micro- or nano-scale regions with different elastic/plastic properties (i.e. soft and hard regions) [9]. The soft regions facilitate shear transition zones nucleation and further shear band initiation, while the hard regions can effectively impede shear bands from propagating catastrophically. The interaction between shear bands and soft/hard regions would induce the formation and branching/arresting of multiple shear bands, accommodating more inelastic strain. In fact, structural inhomogeneity is a natural design in biomaterials [19]. However, up to now, microstructural inhomogeneity in metallic glasses has been realized mainly through composition adjustments [9–13]. This is a trial-and-error routine, which is difficult to control and limited to some special glassy alloys only [5]. Recent computational simulations [20] and experimental results [15,21–23] have shown that deformation and stress field could induce microstructure change of BMGs, shedding light on the possibility of tuning microstructures of BMGs by external stress fields, which can either soften or harden glassy alloys [15,22–24].

Based on the previous results, it is expected that if a correctly designed inhomogeneous stress field can be imposed on a BMG, the structure of the BMG would change accordingly, and structural inhomogeneity and enhanced plasticity might be gained as a consequence. To put the concept into practice, we applied lateral precompression treatments to various BMG rods, and found that the method can easily achieve structural inhomogeneity and effectively plasticize most known BMGs. The match between the scale of structural inhomogeneity and the size of plastic zone of BMGs is a key factor for the plasticity enhancement. Our work further confirms the correlation between the plasticity and the structural heterogeneity in metallic glasses, and has implications for understanding the puzzle of the plastic deformation mechanism of metallic glass.

A series of monolithic BMGs (2 mm in diameter, fabricated by Cu-mold casting [2]) with different compositions listed in Table 1 were chosen for experiment. Uniaxial compression was performed on an Instron-type universal tester with an initial strain rate of $1 \times 10^{-4}\ s^{-1}$ at room temperature. The test samples were cut and polished to a length of 4 ± 0.10 mm. Vickers microhardness test was carried out in an Everone MH-6 microhardness tester, with 100 g load for 15 s. The fractography was observed using a Philips XL 30 scanning electron microscope (SEM). Stress distribution induced by lateral precompression treatment was investigated by the finite element method (ABAQUS software).

* Corresponding author. E-mail: hybai@aphy.iphy.ac.cn

1359-6462/$ - see front matter © 2009 Acta Materialia Inc. Published by Elsevier Ltd. All rights reserved.
doi:10.1016/j.scriptamat.2009.06.005

Table 1. Compressive strength and plasticity for typical BMGs before and after pre-compression treatment; ε, σ denote plasticity and yield strength, respectively; subscripts as and pre denote as-cast and lateral pre-compression treated, respectively; F is the optimum force for ductilizing BMG rod (diameter 2 mm, length 4 ± 0.10 mm).

BMG	ε_{as} (%)	ε_{pre} (%)	σ_{as} (GPa)	σ_{pre} (GPa)	F (kN)
$Cu_{46}Zr_{46}Al_8$	~0.5	4	1.82	1.77	5
$Cu_{60}Zr_{20}Hf_{10}Ti_{10}$	~4	13	2.23	2.14	7
$Zr_{52.5}Cu_{17.9}Ni_{14.6}Al_{10}Ti_5$ (vit105)	~2	10	2.01	1.94	6
$Zr_{46.75}Ti_{8.25}Cu_{7.5}Ni_{10}Be_{27.5}$ (vit4)	~4	16	1.92	1.86	6
$Zr_{41.25}Ti_{13.75}Ni_{10}Cu_{12.5}Be_{22.5}$ (vit1)	~3	18	2.26	1.99	7
$Zr_{65}Cu_{15}Ni_{10}Al_{10}$	~8	12	1.75	1.68	4
$La_{55}Al_{25}Ni_5Cu_{10}Co_5$	<0.1	0.4	0.83	0.80	2.5
$Ce_{60}Cu_{19}Al_{10}Co_1$	<0.1	0.4	0.55	0.52	1.6
$Tm_{39}Al_{25}Co_{20}Y_{16}$	0	0	1.95	1.95	–
$Mg_{65}Cu_{25}Y_{10}$	0	0	0.65	0.65	–

To impose inhomogeneous stress fields, samples were treated by lateral pre-compression, normal to the longitudinal axis, as schematically shown in Figure 1a. Figure 1b presents the microhardness (Hv) distribution of as-cast and the treated $Zr_{52.5}Cu_{17.9}Ni_{14.6}Al_{10}Ti_5$ BMG (vit105), perpendicular and parallel to the lateral pre-compressive direction (defined as X and Y, respectively). The Hv values of the as-cast BMG distribute homogeneously along both X and Y directions, indicating the homogeneous structure of the BMG in tens of μm scale (size of indenter). After the treatment, however, the Hv values of the treated vit105 in the center and brim regions along either the X or the Y direction markedly decrease and deviate from homogeneous distribution in the as-cast state in a parabolic manner (see Fig. 1b). This indicates the lateral pre-compression treatment transforms the homogeneous vit105 into an inhomogeneous structure. The scale of the inhomogeneity is several tens of micrometers, estimated from the microhardness test. This kind of structural inhomogeneity is substantially different from those achieved by composition adjustments [9,10].

The induced structural inhomogeneity has a significant effect on the mechanical properties of BMGs. To illustrate, an example is presented in Figure 2a, in which compression tests of vit105 are taken. It can be seen that when the pre-compressive force is lower than 3 kN or higher than 7 kN, the plasticity enhancement is not distinct. When vit105 is treated with the pre-compressive forces of 4–7 kN, as shown in Figure 2a, its plasticity increases markedly from 1% to an average of 8%, with a maximum of 10.3%. The optimum force for ductilizing vit105 is around 6 kN. Meanwhile, the yield strength of the BMG decreases linearly with applied force as shown in Figure 2b. This implies that larger pre-compressive force would create more soft regions that can result in strength reduction. The evolutions of the strength and compressive plasticity of the BMG with the pre-compressive forces are expected to originate from the evolutions of hard/soft regions, driven by the external stress fields.

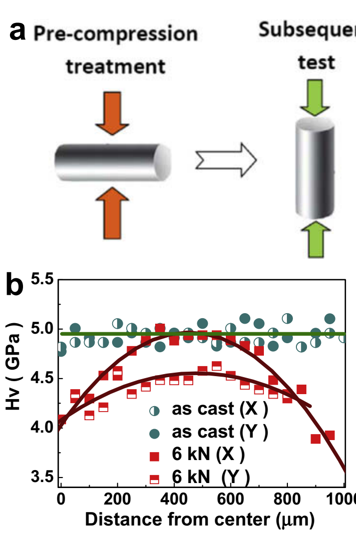

Figure 1. (a) Illustration for the lateral pre-compression treatment and subsequent compression test; solid arrows indicate load directions. (b) Hv distribution along X and Y directions (perpendicular and parallel to the lateral pre-compressive direction) on the cross-section of as-cast and a lateral pre-compressed (6 kN) vit105; the origin point corresponds to the center of the cross-section of the sample. System error of microhardness tester is about 2–3%.

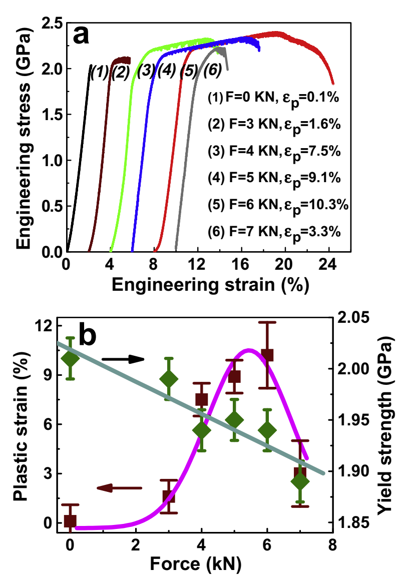

Figure 2. (a) Typical engineering stress–strain curves for as-cast vit105 and subsequent compression of lateral pre-compressed vit105. (b) Compressive yield strength and plasticity as a function of the pre-compressive loads. Each measurement is repeated at least 3 times.

For BMG, the formation and propagation of shear bands account for their plastic flow. Figure 3 shows SEM observations of fractured surface of the treated vit105. For as-cast vit105, with compression plasticity of ~1%, few shear bands on its surfaces can be observed by SEM [25]. However, as shown in Figure 3a, for the vit105 treated by lateral pre-compression 6 kN (subsequent plasticity is ~10%), intensive and network-like shear bands are observed on the sample surfaces before shear strain localizes into one major shear band. The SEM observation confirms that enhanced plasticity is accompanied by massive shear bands formation and branching/arresting [3–5]. The shear bands, which are easily formed on soft regions, would encounter an increasing propagation resistance as it advances in to the hard regions, and induce enhanced plasticity in BMGs [9]. For treated vit105 with a force of 8 kN (subsequent plasticity is ~2%), very few shear bands appear; instead, obvious cracks can be found in zones between the pre-compressed surfaces and the cylindrical free surfaces (Fig. 3b), which indicates too large lateral pre-compressive forces (>7 kN for vit105) induce crack initiation and lead to early fracture on subsequent loading. This explains why the effectiveness of the present method decreases drastically when the pre-compressive force is too large.

To understand the effect of the method, finite element analysis of the lateral pre-compression experiment was performed. Figure 4 presents a typical case for simulated von Mises stress distribution in treated vit105. When the lateral pre-compressive force is less than 4 kN (Fig. 4b), the stress in most part of the sample is small (except the parts near touching surfaces), and the induced structural change is negligible. The magnitude and range of the stress field increases with the pre-compressive force. When the force reaches a critical value, a complex stress pattern is formed on the cross-section of the BMG rod as shown in Figure 4c. The center and brims along the X and Y directions endure larger stress, which softens the material therein [23,24]. The magnitude of stress between center and brims is relatively small, indicating less structural change there [23,24]. The finite element analysis confirms that a "soft–hard" collage-like inhomogeneous structure can be achieved by the lateral pre-compression, which is consistent with the Hv experimental results. With further increase of the pre-compressive loads, more parts of the BMG are affected by the stress fields (Fig. 4d), and more soft regions are created and dominate in the BMG, which leads to easy propagation of shear bands or crack and low plasticity. Therefore, only an optimized combination of soft and hard regions achieved by suitable stress field can effectively ductilize the BMG [9], which is consistent with experimental results.

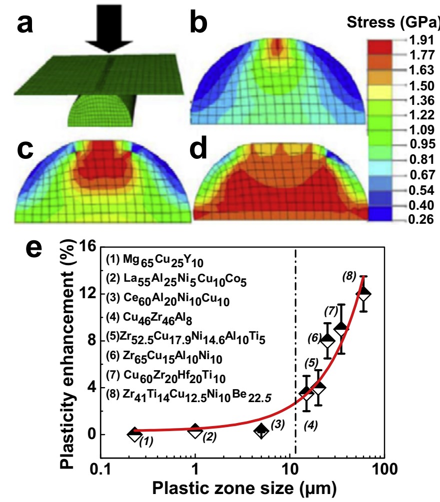

Figure 4. Finite element analysis of vit105 rod under lateral pre-compression: (a) model system; von Mises stress distribution on its cross-section for lateral compressive force of (b) 3 kN, (c) 6 kN and (d) 10 kN. (e) Relationship between plasticity enhancements (defined as enhanced plasticity minus plasticity of as-cast state) and plastic zone sizes (data are taken from Ref. [27]) for different BMGs.

To verify the role of lateral pre-compression treatment in the formation of structural inhomogeneity in the BMG, square (cross-section) shape vit105 plates (1.5 mm×1.5 mm×3 mm) were also treated by this method. However, the effectiveness is not as evident as it is for cylinder BMGs because lateral pre-compression cannot induce distinct stress/structural inhomogeneity in the square shape BMGs, confirming that plasticity enhancements mainly result from stress-induced structural inhomogeneity, rather than other factors such as mechanical and tempering residual stress [15] or pre-formed shear bands [16]. We also applied the treatment to other typical BMG rods, including Zr-, Cu-, Mg- and rare-earth-based BMGs, and the results are listed in Table 1. The treatment can effectively ductilize BMGs from quasi-brittle (e.g. Ce- and La- based) to quasi-ductile (e.g. Zr–Al–Ni–Cu) BMG systems. However, for those very brittle BMGs (e.g. Tm- and Mg-based) its effectiveness is minimal.

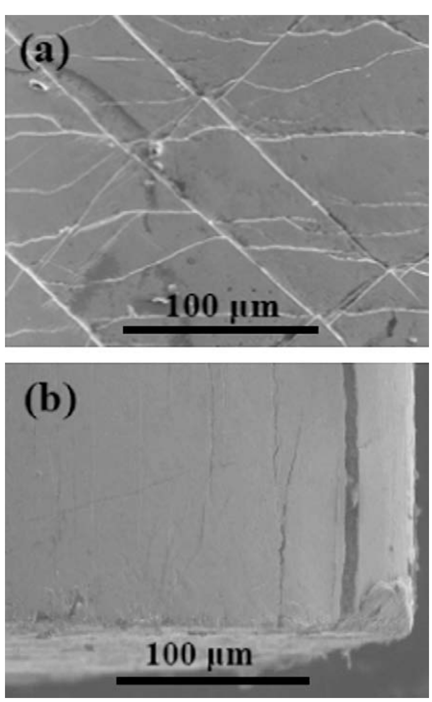

Figure 3. SEM images of compressive fractured and/or shear deformed surfaces of lateral pre-compressed vit105; (a) under force of 6 kN and (b) 8 kN.

The size of plastic zone in front of crack tip is related to fracture toughness [26] and maximum stable shear offset along a shear band in metallic glass [27]. To understand the variation of the effectiveness of the presented method for different BMG systems, the match between the plastic zone in front of the crack tip and the scale of structural inhomogeneity should be considered. It is reported that stability against crack/shear band opening can be ensured when the geometrical size of BMG or structural inhomogeneity scale is approximate to the size of the plastic zone [13]. Figure 4e plots the sizes of plastic zones vs. plasticity enhancements (defined as enhanced plasticity minus plasticity of as-cast state [26]) for different BMGs. It shows that BMGs with plastic zones larger than a critical size of $\sim$10 μm can be potentially ductilized by the presented method, while those with plastic zones smaller than $\sim$10 μm cannot. Based on our results, this implies that the lateral pre-compression method might take effect when the scale of the stress-induced structural inhomogeneity matches the size of the plastic zone of the BMGs. It might be expected that even very brittle BMGs could be ductilized if a method could induce structural inhomogeneity in smaller scales (e.g. submicron/nano-scale inhomogeneity).

In summary, an appropriate inhomogeneous stress field can induce micron-scale structural inhomogeneity in BMGs, and results in macroscopic compressive plasticity improvement when the achieved structural inhomogeneity in a BMG matches its plastic zone in size. Our work is suggestive for designing methods to ductilize BMGs and understanding the deformation mechanism in metallic glasses.

We are grateful to D.Q. Zhao, M.X. Pan, J.S. Gu, P. Yu, M.Q. Jiang and G. Wang for discussions and/or assistances. Financial support is from the NSF of China (Nos. 50671117, 50731008 and 50621061) and MOST 973 (No. 2007CB613904).

[1] A.L. Greer, Science 267 (1995) 1947.
[2] W.H. Wang, Prog. Mater. Sci. 52 (2007) 540; W.H. Wang, J Appl. Phys. 99 (2006) 093506.
[3] A.R. Yavari, J.J. Lewandowski, J. Eckert, MRS Bull. 32 (2007) 635.
[4] C.A. Schuh, T.C. Hufnagel, U. Ramamurty, Acta Mater. 55 (2007) 4067.
[5] M.W. Chen, Annu. Rev. Mater. Res. 38 (2008) 14.
[6] D.M. Dimiduk, C. Woodward, R. LeSar, M.D. Uchic, Science 312 (2006) 1188.
[7] W.J. Wright, R.B. Schwarz, W.D. Nix, Mater. Sci. Eng. A 319 (2001) 229.
[8] J. Schroers, W.L. Johnson, Phys. Rev. Lett. 93 (2004) 255506.
[9] Y.H. Liu, G. Wang, R.J. Wang, D.Q. Zhao, M.X. Pan, W.H. Wang, Science 315 (2007) 1385.
[10] M.B. Tang, W.H. Wang, Chin. Phys. Lett. 21 (2004) 901; J. Das, M.B. Tang, K.B. Kim, W.H. Wang, J. Eckert, Phys. Rev. Lett. 94 (2005) 205501.
[11] G. Wang, Y.H. Liu, M.X. Pan, W.H. Wang, Appl. Phys. Lett. 89 (2006) 251909.
[12] D.G. Pan, H.F. Zhang, Z.Q. Hu, Appl. Phys. Lett. 89 (2006) 261904.
[13] P. Wesseling, T.G. Nieh, W.H. Wang, J.J. Lewandowski, Scripta Mater. 51 (2004) 151.
[14] P. Yu, H.Y. Bai, J.G. Zhao, W.H. Wang, Appl. Phys. Lett. 90 (2007) 051906.
[15] Y. Zhang, W.H. Wang, A.L. Greer, Nat. Mater. 5 (2006) 857.
[16] L. He, M.B. Zhong, F. Jiang, J. Sun, Mater. Sci. Eng. A 496 (2008) 285.
[17] W.F. Wu, C.Y. Zhang, Y.W. Zhang, K.Y. Zeng, Y. Li, Intermetallics 16 (2008) 1190.
[18] K.F. Yao, C.Q. Chen, Appl. Phys. Lett. 90 (2007) 061901.
[19] M.A. Meyers, P. Chen, A.Y. Lin, Y. Seki, Prog. Mater. Sci. 53 (2008) 1.
[20] Y.Q. Cheng, A.J. Cao, H.W. Sheng, E. Ma, Acta Mater. 56 (2008) 5263.
[21] K.W. Park, C.M. Lee, M. Wakeda, Y. Shibutani, M.L. Falk, J.C. Lee, Acta Mater. 56 (2008) 5440.
[22] L.Y. Chen, Q. Ge, S. Qu, J.Z. Jiang, Scripta Mater. 59 (2008) 1210.
[23] S. Xie, E.P. George, Acta Mater. 56 (2008) 5202.
[24] F. Spaepen, Acta Metall. 25 (1977) 407.
[25] Z.F. Zhang, J. Eckert, L. Schultz, Metall. Mater. Trans. A 35 (2004) 3489.
[26] X.K. Xi, D.Q. Zhao, M.X. Pan, W.H. Wang, Y. Wu, J.J. Lewandowski, Phys. Rev. Lett. 94 (2005) 125510.
[27] G. Ravichandran, A. Molinari, Acta Mater. 53 (2005) 4087.